HHS Public Access

Author manuscript

Dev Comp Immunol. Author manuscript; available in PMC 2016 November 01.

Published in final edited form as:

Dev Comp Immunol. 2015 November ; 53(1): 158–168. doi:10.1016/j.dci.2015.07.002.

Retention of duplicated ITAM-containing transmembrane signaling subunits in the tetraploid amphibian species *Xenopus laevis*

S.V. Guselnikov[a,b], **L. Grayfer**[c], **F. De Jesús Andino**[c], **I.B. Rogozin**[d], **J. Robert**[c], and **A.V. Taranin**[a,b,*]

S.V. Guselnikov: sguselnikov@mcb.nsc.ru; L. Grayfer: Leon_Grayfer@urmc.rochester.edu; F. De Jesús Andino: f_dejesus7@yahoo.com; I.B. Rogozin: rogozin@ncbi.nlm.nih.gov; J. Robert: Jacques_Robert@urmc.rochester.edu; A.V. Taranin: taranin@mcb.nsc.ru

[a]Institute of Molecular and Cellular Biology, Siberian Branch of the Russian Academy of Sciences, Lavrentiev Avenue 8/2, Novosibirsk 630090, Russia

[b]Novosibirsk State University, Pirogov Street 2, Novosibirsk 630090, Russia

[c]University of Rochester, Medical Center, 601 Elmwood Avenue, MRBX, Rochester, NY 14642, USA

[d]National Center for Biotechnology Information NLM, National Institutes of Health, 8600 Rockville Pike, Bldg. 38A, Bethesda, MD, USA

Abstract

The ITAM-bearing transmembrane signaling subunits (TSS) are indispensable components of activating leukocyte receptor complexes. The TSS-encoding genes map to paralogous chromosomal regions, which are thought to arise from ancient genome tetraploidization(s). To assess a possible role of tetraploidization in the TSS evolution, we studied TSS and other functionally linked genes in the amphibian species *Xenopus laevis* whose genome was duplicated about 40 MYR ago. We found that *X. laevis* has retained a duplicated set of sixteen TSS genes, all except one being transcribed. Furthermore, duplicated TCRα loci and genes encoding TSS-coupling protein kinases have also been retained. No clear evidence for functional divergence of the TSS paralogs was obtained from gene expression and sequence analyses. We suggest that the main factor of maintenance of duplicated TSS genes in *X. laevis* was a protein dosage effect and that this effect might have facilitated the TSS set expansion in early vertebrates.

Keywords

Xenopus; Genome mining; Activating receptor complexes; TCR; Tetraploidization; Protein dosage effect; Immunogenetics

*Corresponding author. Address: IMCB SB RAS, 8/2 Lavrentiev Avenue, Novosbiirsk 630090, Russia.

1. Introduction

Leukocyte activation is generally mediated by cell surface receptor complexes composed of two functionally different types of subunits (Humphrey et al., 2005). The ligand binding subunits interact with extracellular self or non-self ligands. These molecules often have short cytoplasmic tails with limited or no signaling ability. The interaction signal from such receptor complexes is transmitted to the intracellular machinery through a second type of subunits, which are called transmembrane adapter or signaling subunits (TSS).

Mammalian species have nine different TSS molecules. Five of them are characterized by the presence of an extracellular Ig-like domain and specific association with TCR (CD3ε, CD3γ, CD3δ) or BCR (CD79a, CD79b). Four other TSS are FcRγ, TCRζ/CD3ζ, DAP12/TYROBP/KARAP and DAP10. These adapter subunits possess only short extracellular regions and associate with a variety of functionally distinct receptors expressed on different cell subsets. Because of their involvement in key receptor complexes, TSS molecules are indispensable for immune functions. Deficiency in these molecules profoundly affects the organism's ability to mount both innate and adaptive immune responses (Ivashkiv, 2009; Colonna, 2003; Niiro and Clark, 2002; Malissen et al., 1999; Shores et al., 1998; Takai et al., 1994).

The signaling properties of all TSS molecules except DAP10 are determined by the immunoreceptor tyrosine-based activation motifs (ITAM) in their cytoplasmic tails (Reth, 1989). The CD3, CD79b, FcRγ, and DAP12 subunits each contain a single classical ITAM conforming to the consensus D/E/NxxYxxL/I-$(x)_7$-YxxL/I, whereas TCRζ has three such motifs. The intracellular region of CD79a has three YxxL/I modules separated by seven-residue spacers. Finally, DAP10 has a unique tyrosine-based motif with a methionine residue (YINM/IMNV/IMNT). The classical ITAM is always encoded by two exons with the exon boundary splitting the first tyrosine module. All TSS molecules have a negatively charged residue in their transmembrane (TM) regions. This residue facilitates non-covalent assembly with ligand-binding chains, which usually contain a positively charged residue in their TMs (Call et al., 2010). Recent data suggest that additional cell surface molecules, generally not considered as immunoreceptors, may depend on TSS for proper signaling (Hamerman et al., 2009).

The subdivision of activating immunoreceptors into ligand-binding and signaling subunits is a basic characteristic of the immune system of jawed vertebrates. For this reason, understanding how and when the TSS set might have emerged is important for understanding the evolution of adaptive immunity. At present, little is known about the TSS ancestry. What is clear is that, in contrast to their ligand-binding partners, the ITAM-containing subunits are highly conserved. The set of eight TSS genes in the teleost pufferfish is very similar to that of mammals (Guselnikov et al., 2003b). The duplication of the ancestral *CD3γ/δ* gene into *CD3γ* and *CD3δ* seems to be the only important mammalian acquisition compared to Teleosts. Based on the sequence homology and chromosomal localization, we have proposed that the primordial set of TSS genes comprised four members: CD3-like, CD79-like, FcRγ/TCRζ-like and DAP10/DAP12-like (Guselnikov et al., 2003b). Furthermore, it is noteworthy that TSS genes map to the chromosomal regions

regarded as paralogons in several vertebrate species (Zucchetti et al., 2009). In the human genome, these are 1q23-24 (*TCRζ* and *FcRγ*), 11q23 (*CD3ε,δ,γ*), and 19q13 (*DAP10*, *DAP12*, *CD79a*). Such localization of the TSS genes raises the interesting possibility that they might have emerged from a common ancestor through ancient tetraploidization events, which are thought to have occurred in the early evolution of jawed vertebrates.

That the whole genome duplications (WGD) may result in the expansion and diversification of the TSS set is supported from studies of several fish species. Yoder et al. (2007) have demonstrated that zebrafish has two *FcRγ* and two *TCRζ* genes. The duplicated genes are highly diverged and differentially expressed, suggesting their functional specialization. The chromosomal regions containing the paralogous genes have been predicted to be a result of the teleost-specific tetraploidization. The *FcRγ* and *TCRζ* duplicates have also been found in catfish (Mewes et al., 2009). The duplication of CD3 genes in sterlet (Alabyev et al., 2000) and Atlantic salmon (Liu et al., 2008) is also noteworthy, especially since both of these species belong to lineages that have recently undergone tetraploidization.

To gain deeper insight into the post-WGD evolution of the TSS set, we examined the structure and expression of the TSS genes in two related amphibian species *Silurana (Xenopus) tropicalis* and *Xenopus laevis*. These species are thought to have separated approximately 65 MYR ago (Evans, 2008). Both are prominent experimental models differing in the genome ploidy. *Silurana tropicalis* is a diploid species, whereas the *X. laevis* genome has been allotetraploidized some 21–41 MYR ago (Evans, 2008). There is not much evidence for the persistence of WGD-derived copies of immune system genes in *X. laevis*. The experimental data have demonstrated the presence of a single locus for IgH, TCRβ, MHC class I and Class II genes (Courtet et al., 2001; Chretien et al., 1997; Shum et al., 1993). A biochemical study of the *X. laevis* TCR complex did not reveal much heterogeneity among molecules co-precipitated with antibodies against chicken CD3ε (Gobel et al., 2000). A single *CD3γ/δ* gene has been described in this species (Dzialo and Cooper, 1997). At the same time, genomic blot hybridization suggested the presence of two *FcRγ* and *TCRζ* genes (Guselnikov et al., 2003a).

The recent sequencing of the *S. tropicalis* (Hellsten et al., 2010) and *X. laevis* genomes (www.xenbase.org) made it possible to compare the genes of the two species in more detail. Here, we have studied how TSS and some TSS-associating genes have evolved after tetraploidization in the *Xenopus* lineage. It was found that *X. laevis* has a double set of the TSS genes. The duplicated genes are localized on the duplicated genomic regions. One of the *CD3γ/δ* paralogs is aberrant. Fifteen other TSS genes have no apparent aberrations and are transcribed. Notably, the *X. laevis* genome also retained the WGD-derived *TCRα* loci and genes for TSS-coupled tyrosine protein kinases, such as Syk, ZAP70, and PI3K. The data obtained suggest that protein dosage effects played and still play a role in the retention of the *X. laevis* TSS paralogs. These findings also favor the idea that the TSS set may have expanded through ancient WGD(s) in emerging jawed vertebrates.

2. Materials and methods

2.1. Similarity search and gene prediction

Sequence similarity searches were performed using the TBLASTN and BLASTP programs on the NCBI site (http://www.ncbi.nlm.nih.gov/). The nucleotide and amino acid sequences of mammalian, amphibian, and fish TSS cDNAs were retrieved from GenBank using ENTREZ on the same site. The genomic sequences of *Xenopodinae* TSS sequences were retrieved from the Xenbase (http://www.xenbase.org/, James-Zorn et al., 2013) and Ensembl (http://www.ensembl.org/) websites. Structure of *X. laevis* and *S. tropicalis* TSS genes was predicted based on the structure of mammalian TSS genes, available EST sequences and gt-ag rule. Surrounding genes were identified using utilities on the Xenbase and Ensembl sites and were verified by reciprocal sequence comparisons at the NCBI website using the BLASTP program.

2.2. Sequence alignment and phylogenetic analysis

Amino acid sequences were aligned using Clustal utilities of the MEGA4 software (Tamura et al., 2007) and shaded manually according to Timberlake classification of amino acids (Timberlake, 1992). Phylogenetic analysis was performed with the MEGA4 software using nucleotide sequences aligned based on the alignment of amino acid sequences. In certain cases, the CLUSTAL generated alignments were manually corrected. Phylogenetic trees were constructed using the bootstrap and interior branch tests of the Neighbor-joining (NJ) method with p-distances (proportion of differences). Minimum Evolution (ME) trees were essentially the same as the NJ trees in the major branching patterns.

2.3. Estimation of the rates of non-synonymous substitutions

The RRTREE program was used to estimate the rates of non-synonymous substitutions (Ka, the PBL model) (Robinson-Rechavi and Huchon, 2000) between the pairs of *X. laevis* paralogous TSS genes. *S. tropicalis* orthologs were used as outgroup sequences.

2.4. Experimental animals

Adult outbred *X. laevis* were obtained from the *X. laevis* Research Resource for Immunobiology at the University of Rochester Medical Center (www.urmc.rochester.edu/smd/mbi/xenopus/index.htm). Animals were euthanized with 0.5% Tricainemethanesulfonate (TMS). All of the animals were handled under strict laboratory and UCAR regulations (Approval number 100577/2003-151) minimizing animal suffering at all times.

2.5. RT-PCR

Tissue samples were homogenized in 0.8 mL of Trizol reagent (Invitrogen). Total RNA was extracted according to the manufacturer's protocol and quantified with Nanodrop 2000 (Thermo Scientific). 2 μg of total RNA were used to synthesize cDNA with iScript first strand cDNA synthesis kit (BioRad) according to the manufacturer's protocol. The cDNA samples were diluted to a final volume of 50 μl and then PCR amplification was performed. For each standard 30 μl PCR reaction 1 μl of cDNA and 1 U of Taq DNA polymerase (Life

Technologies) were used. The reaction condition was as follows: (95 °C – 30 s, 60–64 °C – 30 s and 72 °C – 30 s) × 30–35 cycles. All cDNA samples were further normalized based on the actin or *GAPDH* expression level. Primers for different exons were used to neglect a genomic DNA contamination (for details, see Supplementary data 1, f and r primers).

RT-PCR products from the primer pairs flanking the CDS of DAP10.b, CD3ε.b, CD79a.a, CD79a.b and CD79b.b (Supplementary data 1, f2 and r2 primers) were obtained from the same cDNA samples using Phusion proof-read DNA polymerase (Finnzymes), ethanol-precipitated and sequenced on both strands. These sequences were deposited in GenBank with accession numbers KT223646, KT163019, KT163020, KT163021 and KT223647, respectively.

2.6. cDNA library screening: TcRζ.b

cDNA library from a spleen of an adult *X. laevis* was screened with TcRζ.a-specific probe (Guselnikov et al., 2003a) as described in Guselnikov et al., 2008. Individual TcRζ.a and TcRζ.b cDNA clones were isolated and sequenced. A representative TcRζ.b sequence was deposited in GenBank under accession number EF431896.

2.7. DAP12.b EST cDNA clone sequencing

X. laevis EST cDNA IMAGE:5506074 was purchased from the ATCC consortium and sequenced on both strands. The sequence for the full CDS of DAP12.b was deposited in GenBank under accession number EF431894.

2.8. Co-expression of X. laevis XFL2 receptor and FcRγ subunits in eukaryotic 293T cells

XFL2 cDNA was cloned into pDisplay vector (Invitrogen) as described previously (Guselnikov et al., 2008). In addition, the complete coding regions of *X. laevis* FcRγ.a (AF499689) and FcRγ.b cDNAs (EF431895) were cloned into pAP-Tag5 vector (GenHunter). As a result, these constructions encoded XFL2 receptor with N-terminal HA epitope and FcRγ subunits with c-myc epitope at their C-end. 293T cells were transiently transfected with the plasmids. Transfections were carried out using Unifectin 56 (IBCH, Moscow, Russia) according o the manufacturer's protocol. After 72 h transfection, the cells were used for immunocytochemistry and flow cytometry. The surface expression of XFL2 was analyzed with FACSCanto II cytometer (BD Bioscience): live cells were stained with mouse monoclonal 12CA5 anti-HA antibody (Abcam) and goat anti-mouse Ig-FITC (BD Bioscience). Intracellular expression of FcRγ subunits was detected using microscope Axioscop 2 plus (Carl Zeiss): transfected cells were smeared on glass slides, fixed with acetone and stained with anti-c-myc 9E10 monoclonal antibodies (Abcam) and goat anti-mouse IgG-Tex-asRed (Molecular Probes).

3. Results

3.1. The TSS genes are duplicated in the X. laevis genome

We performed a TBLASTN search of the genomic and cDNA sequences of *X. laevis* and its diploid relative *S. tropicalis* on the Xenbase (www.xenbase.org) and Ensemble (www.ensembl.org) sites using known TSS sequences. The search revealed a single gene for

each TSS in the *S. tropicalis* genome and two genes for each TSS in the *X. laevis* genome. Following the guidelines of the Xenopus Gene Nomenclature Committee (www.xenbase.org/gene/static/geneNomenclature.jsp), the duplicated *Xenopus* genes were designated “a” and “b”. We tentatively gave an “a” symbol to those four *X. laevis* TSS genes that have already been described at the nucleotide or amino acid levels. These are *CD3γ/δ* (Dzialo and Cooper, 1997), *FcRγ*, *TCRζ*, and *DAP10* (Guselnikov et al., 2003a, 2003b). Their duplicates were designated as “b” variants.

Next, we compared the scaffolds with the duplicated TSS genes and found them to represent duplicated genomic regions (Fig. 1). As it is known, there is a close linkage between *DAP10* and *DAP12*, as well as between *CD3ε* and *CD3γ/δ* genes in the mammalian and fish genomes. These linkages are maintained in *S. tropicalis* and in the duplicated regions of the *X. laevis* genome. We have previously noted the conserved linkage of the TSS genes with *EVA1/MPZL2* (*CD3ε* and *CD3γ/δ*), *ARHGEF1* (*CD79a*), *SCN4A* (*CD79b*), *NFKBID* (*DAP10* and *DAP12*), *NDUFS2* (*FcRγ*) and *CREG1* (*TCRζ*) in the human and pufferfish genomes (Guselnikov et al., 2003b). The duplicated copies of these and some other genes were mostly retained in the *X. laevis* genomic fragments containing the TSS gene paralogs (Fig. 1). However, the gene sizes, intergenic distances and, in some cases, the gene content on these scaffolds were different. This pattern is compatible with the WGD that have occurred some dozens of MYR ago. With the exception of *CD3γ/δ.b*, the sequence analysis of all the other *X. laevis* TSS gene models did not reveal any error or aberration. Examination of the *CD3γ/δ.b* gene model revealed stop codons in the exons coding for the extracellular domain and signal peptide. In addition, we did not find exon for the TM region. Hence, we considered *CD3γ/δ.b* as a pseudogene. The predicted models for the rest TSS genes were confirmed by the structure of the corresponding cDNAs (Supplementary data 2).

The exon-intron structure of the *Xenopus* TSS genes is generally similar their mammalian counterparts (Figs. 2 and 3). The only notable difference is the structure of the FcRγ genes. Instead of 5 exons in the mammalian and teleost counterparts, both *X. laevis* FcRγ genes contain 6 exons. At the deduced amino acid level, the presence of an additional exon results in the emergence of the second ITAM motif in the cytoplasmic tail, a unique feature of *X. laevis* FcRγ that we have described previously (Guselnikov et al., 2003a). Like the classical ITAM, this additional motif is encoded by two exons with the exon border in the first tyrosine-based module.

Phylogenetic trees generated on the basis of nucleotide sequences of TSS clearly demonstrated that the *X. laevis* duplicates are closer to each other than to their *S. tropicalis* homologs (Supplementary data 3). The tree topology was mostly tolerant to changes in settings and methods used for the tree generation. These results suggest that duplications of *X. laevis* genes occurred after the speciation of *X. laevis* and *S. tropicalis*.

Alignments of the deduced amino acid sequences of the *X. laevis* TSS duplicates with each other and with their mammalian homologs are shown on Figs. 2 and 3. The similarity between the duplicated copies of *X. laevis* TSS ranged from 72% (CD79a) to 88% (TCRζ) identical residues. In the case of CD3ε, CD79a and CD79b, the divergence mostly affected the extracellular domains. These domains are known to stabilize the respective TCR and

BCR complexes by interacting with the membrane-proximal domains of the respective ligand-binding chains (Radaev et al., 2010; Kuhns and Davis, 2007). The sequence comparisons showed that the extra-cellular domains of *X. laevis* CD79b.a and CD79b.b differ from each other and from other species CD79b in the number of cysteine residues. This feature may differentially affect their homodimerization, their heterodimerization with CD79a and, ultimately, their association with the Ig chains according to the data obtained in the studies of mammalian CD79 subunits (Radaev et al., 2010).

The known critical residues in the TM and cytoplasmic regions of CD3ε/γδ and CD79a/b are identical. Comparison of the DAP12 duplicates shows their high sequence similarity. The DAP10 copies are also highly similar except for the distal C-terminal. The Cyt region of DAP10.a is shorter because of the acquisition of a premature stop-codon in the 3′-terminal exon. Finally, comparisons of TCRζ and FcRγ copies demonstrate an accumulation of differences in their Cyt regions, namely in the first ITAM of TcRζ and second ITAM of FcRγ.

Gene duplication is widely regarded as a major mechanism modeling genome evolution and function (Rogozin, 2014; Fernández et al., 2011; Innan and Kondrashov, 2010; Chain and Evans, 2006; Lynch and Conery, 2000; Hughes, 1994). An important question was whether the differences observed between TSS paralogs might be of functional significance. It is known that functional divergence of gene duplicates is associated with a significantly increased protein sequence divergence after duplication in only one of the copies (Pegueroles et al., 2013). We used the RRTREE program to compare the rates of non-synonymous substitutions (estimated using the PBL model) (Robinson-Rechavi and Huchon, 2000) between pairs of *X. laevis* duplicated genes. No significant rate variations of non-synonymous substitutions were observed for *X. laevis* duplicated genes (Table 1). This result suggests that duplicated copies are unlikely to have major functional differences.

3.2. Expression patterns of the X. laevis TSS paralogs are similar

To further assess the expression patterns of the duplicated genes we performed RT-PCR analysis of mRNA from the spleens of several *X. laevis* adults using copy-specific primers. The results revealed similar expression of both paralogs of the TSS genes examined (Fig. 4). Thereafter, we performed a more detailed RT-PCR analysis of the duplicated *FcRγ* and *TCRζ* genes. We used cDNA from a range of tissues taken from animals at three developmental stages: tadpoles, metamorphs and adults. Three individuals at each stage were examined. The data obtained indicate that *FcRγ.a* and *b* genes are actively transcribed in all tissues studied with the highest level of expression in the spleen and the lowest (or undetectable) in skeletal muscles (Fig. 5). The *FcRγ.a* and *FcRγ.b* gene expression patterns were very similar among adult individuals with respect to the tissue examined and intensity of the RT-PCR bands (Fig. 5A). In tadpoles, one animal showed the decreased expression of *FcRγ.a* in the liver, whereas another frog showed expression of both genes in skeletal muscles (Fig. 5B). More variation in the intensity of the RT-PCR bands was observed in metamorphs. However, these variations were individual and could not be attributed to a consistent difference in the expression of the two genes (Fig. 5C).

Expression analysis of the *TCRζ* genes demonstrated even more individual variability in the band intensity. In adults, both *TcRζ* genes showed expression limited mainly to thymus, spleen, and intestine (Fig. 5A). These data matches perfectly with Northern blot results we have obtained previously (Guselnikov et al., 2003a). Similar expression patterns were observed in tadpole tissues, with *TcRζ.a* and *b* showing prominent expression only in thymus, spleen and gills (Fig. 5B). Metamorphic froglets showed variable patterns for *TcRζ.a* and *TcRζ.b*. Thus, metamorph 1 showed *TCRζ.a* expression in thymus and spleen, whereas *TcRζ.b* was detected in a range of tissues including kidney, liver, gills and fat body. Metamorphs 2 and 3 demonstrated broad expression patterns for both *TcRζ.a* and *TcRζ.b* gene copies (Fig. 5C).

3.3. FcRγ.a and b similarly facilitate XFL2 cell surface expression

Previously, we have reported that the surface expression of XFL2 protein, a member of the *X. laevis* FCRL family, is dependent on co-expression with FcRγ.b. These data suggest that the two proteins interact and form a receptor complex (Guselnikov et al., 2008). As FcRγ.a and FcRγ.b subunits possess identical TM regions, we expected the FcRγ.a to have similar properties. To test this assumption, we transiently transfected 293T cells with the constructions expressing *X. laevis* HA-tagged XFL2 and c-myc-tagged FcRγ.a and FcRγ.b. FACS analysis showed that XFL2 in the absence of TSS remained intracellular, whereas co-expression with any of the two FcRγ subunits resulted in the transport of the receptor to the cell surface (Fig. 6). There were similar values for the percentages of cells expressing XFL2 at their surface (15.3% and 15.8% positive cells) and intracellulary (24% and 27%), as well as for subunit intracellular expression (~25% and ~20%) in the co-transfections with FcRγ.a and FcRγ.b, respectively.

3.4. Two TCRa loci in X. laevis

The retention of duplicated TSS genes in *X. laevis* raised a question as to whether duplicates of genes encoding the associating ligand-binding chains were retained as well. We compared the exact structure of the *IgH*, *TCR* and *LRC* loci in the two species, and also made rough estimates of the number of genes in the FCRL and SLAM gene families in the two species. The results are summarized in Fig. 7 and Supplementary data 4. First of all, in agreement with the available experimental data (Courtet et al., 2001), we found that the current version of the *X. laevis* genome contains a single *IgH* locus. Like in *S. tropicalis* (Zhao et al., 2006), the *X. laevis IgH* locus includes five *CH* genes: μ, δ, χ, ε, and φ (Supplementary data 4).

The CD3 and TCRζ chains are known to associate with TCR and pre-TCR dimers. We found a single pre-*TCRα* gene in both amphibian species (Supplementary data 4). Analysis of the *TCR* genes demonstrated the presence of three *TCR Cα* genes, three *TCR Cδ* genes and a single gene for each of the *Cγ* and *Cβ* regions in the *X. laevis* genome. The presence of a single *TCR Cβ* and two *TCR Cα* genes in *X. laevis* is in agreement with experimental data of Chretien et al. (1997) and Haire et al. (2002), respectively. As to the *TCR Cγ*, our findings contradict the suggestions made on the basis of genomic hybridization (Haire et al., 2002). The contradiction may be explained by the gaps in the current assembly of the *X. laevis* genome. However, based on EST database analysis, we favor the possibility that *X. laevis* possesses a single *TCR Cγ* locus. The *TCRA* locus of diploid *S. tropicalis* has been recently

described by Parra et al. (2010). It occupies roughly 600 kb and is flanked by the *METTL3* and *SALL2* genes on the 5′side and by *DAD1* and *ABHD4* on the 3′side. Apart from a large group of the *V* and *J* segments, the locus includes *Cα1*, *Cα2*, *Cδ1* and *Cδ2* genes; all of them expressed. Its unusual feature is the presence of a cluster of *Vh*-like genes associated with and used by the *Cδ1* gene (Parra et al., 2010). In the *X. laevis* genome (version 7.1), we mapped the *TCRα* and δ genes to five scaffolds: 29869, 41767, 61078, 139621, and 272406. Examination of their content showed that the scaffold 272406 represents the 5′-portion of the *TCRA* locus with *METTL3* and *SALL2* and two closely related *Cδ1*-like genes of which one appears to be a pseudogene (Fig. 7). These genes we designated *Cδ1* and *Cδ1ψ* are likely a result of the *X. laevis*-specific tandem duplication. Similarly to *S. tropicalis*, the *X. laevis Cδ1* gene is linked to a group of *Vh*-like genes. The scaffold 41767 contains the middle portion of *TCRA* locus with *Cα2*-and *Cδ2*-like genes. The scaffold 29869 appears to represent a 3′portion of the locus. It contains a *Cα1*-like gene that we designated *Cα1.a*, the *DAD1*-and *ABHD4*-like genes and a large cluster of *Vh* genes that appears to be a part of the *IgH* locus judging by the EST analysis (not shown). Linkage of the *TCRα* and *IgH* loci has been demonstrated in the *S. tropicalis* genome as well (Parra et al., 2010). The 139621 scaffold is paralogous to the 29869. It contains 8 *Vα* genes as well as *Cα1.b*, *DAD1*, *ABHD4* and *ZMYM1*. The latter gene (*ZMYM1*) is present in a single copy in *X. laevis*. In the *S. tropicalis* genome its position is between the *IgCh* and *Vh* genes (not shown). The deduced amino acid sequences of *Cα1.a* and *Cα1.b* share 72% identical residues and they are 40% identical to *Cα2*. Comparison of the *X. laevis Cα1.a* and *Cα1.b* with *S. tropicalis Cα1* showed 61% and 67% identity, respectively. Finally, the scaffold 61078 was found to contain 12 *Vα* genes as well as copies of *SALL2* and *TOX4* genes, and seems to represent a paralogon of the region in the scaffold 272406. The *Cα1.a* and *Cα1.b* genes appear to be functional as they encode two variants of *X. laevis TCR Cα* cDNAs described by Haire et al. (2002). Their transcripts are abundant in the EST database as well. According to the EST data, the *X. laevis Cδ1* and *Cδ2* are also rearranged and transcribed. Furthermore, the analysis of mRNA representing rearranged genes shows that the scaffolds 29869, 41767, and 272406 are parts of the same *TCRα/δ* locus (not shown). Its structure and gene content are very similar to those in the *S. tropicalis* genome. The scaffolds 139621 and 61078 form another truncated locus that lacks *Cδ*, *Vδ* and *Vh* genes. Based on the presence of the *SALL2*, *TOX4*, *DAD1*, and *ABHD4* paralogs, these two loci most probably were generated in the course of WGD.

We did not find transcripts for *Ca2* gene among the known *X. laevis* nucleotide sequences. This gene model lacks apparent errors except for the absence of the exon encoding the membrane-proximal hinge that is common for TCR chains. Interestingly, the *S. tropicalis Cα2* gene also lacks this exon but is nevertheless transcribed. At the amino acid level, the *S. tropicalis* and *X. laevis Cα2* domains show 77% identity. This degree of similarity is close to that demonstrated by comparisons of the other TCR chains and, therefore, suggests functionality. If the amphibian *Cα2* genes are functional, the TCR chains they encode probably function in a form that differs from conventional disulfide-linked heterodimers.

To assess the number of FcRγ-associated proteins we searched for the exons encoding TMs with the NxxR motif. This TM subtype appears to be the most conserved element of *LRC*

and it has been shown to promote association with FcRγ in different species. In mammals, the NxxR-containing TM is a feature of activating LILRs, NCR1, GPVI, FcαR, and OSCAR (reviewed in Barrow and Trowsdale, 2008), in birds it has been found in *LRC* homolog ggFcR (Viertlboeck et al., 2009). Our previous studies of the *S. tropicalis* genome have shown that NxxR-containing TMs are characteristic for not only *LRC* members but also for members of the expanded FCRL and CD2/SLAM families. Overall, we have found 49 exons coding for the NxxR-containing TMs in the *S. tropicalis* genome (Guselnikov et al., 2011, 2010, 2008). In the *X. laevis* genome, our search revealed 50 such exons.

We next compared the structure of *LRC* in the two species. The *S. tropicalis LRC* locus is represented by four tightly linked genes (*ILR1-ILR4*) encoding receptors with NxxR motif containing TMs (Guselnikov et al., 2010). In the *X. laevis* genome there are two *LRC* loci (Supplementary data 4). The first on the scaffold 29769 contains *ILR1*, *ILR2*, *ILR4* and an aberrant *ILR3*. The second *LRC* locus on the scaffold 139764 has a copy of *ILR2* and an *ILR3*-like gene whose functionality is questionable as it consists of only two exons for the extracellular Ig-like domains. More importantly, both scaffolds also contain copies of the *LRC*-linked genes *TTYH1*, *RPS9* and *CDC42E5* and, for this reason, may be regarded as retained WGD products. Despite the retention of two loci, the *X. laevis LRC* is not much different from *S. tropicalis LRC* in gene number. Altogether, the data obtained in our analysis favors the suggestion that, following the *X. laevis*-specific WGD, the gene families encoding conventional TSS-associating receptors were mostly reduced in size by diploidization. This conclusion is in agreement with observations reported by Ohta et al. (2006) and Flajnik et al. (2012).

3.5. The duplicated X. laevis genes for TSS-coupled protein kinases are retained

The TSS signaling depends on coupling with downstream intracellular signaling cascades. The phosphorylation of TSS ITAMs generates docking sites for the intracellular protein kinases ZAP70 (CD3/TCRζ), Syk (CD79a/b), Lck (FcRγ) or PI3K (DAP10). Search in the *X. laevis* genome for the genes encoding these kinases demonstrated the presence of two genes for ZAP10, Syk, and PI3K. The duplicated genes are localized on distinct scaffolds (Supplementary data 4). The available versions of the *X. laevis* genome lack any *LCK* genes. This is apparently due to the gaps in the current assemblies as a cDNA for *X. laevis* homolog of *LCK* is present in the *X. laevis* collection of full-length cDNAs (not shown). Furthermore, conserved recognition site for the p56lck with the consensus sequence motif ‘RXCQC’ have described for *Xenopus* CD4 (Chida et al., 2011).

4. Discussion

Here, we show that the allotetraploid amphibian species *X. laevis* possesses a duplicated set of TSS genes. According to our phylogenetic analysis, the duplications took place after the radiation of the *X. laevis* and *S. tropicalis* lineages. This finding together with the structure and gene content of the scaffolds bearing the TSS genes strongly suggests that the duplication resulted from the allotetraploidization of the *X. laevis* genome, which is estimated to have happened 21 to 41 MYR ago (Chain and Evans, 2006). Without experimental data on chromosome localization we cannot formally exclude segmental duplications in the studied loci. However, this latter mechanism seems rather improbable as

it implies many additional events, such as the loss of the duplicated loci after tetraploidization and their subsequent simultaneous *de-novo* gain. The long-term maintenance of duplicated genes is generally explained in two ways. First, the paralogs may be retained because of their rapid functional divergence. This includes the classical neofunctionalization (Ohno, 1970) or various types of sub-functionalization (Fernández et al., 2011; Innan and Kondrashov, 2010; Chain and Evans, 2006; Lynch and Conery, 2000; Hughes, 1994). An alternative mechanism is that duplicated genes may be retained because of a beneficial protein dosage effect (Kondrashov et al., 2002). According to this latter model, the dosage-based long-term persistence of functionally identical paralogs allows their structural divergence and increases the probability of sub- or neofunctionalization.

We did not find evidence favoring the functional divergence of the *X. laevis* TSS paralogs. No significant rate variations of non-synonymous substitutions were observed for these genes (Table 1). The TM regions of duplicates are highly conserved making unlikely their differential association with ligand-binding subunits. At least in the case of FcRγ, a similar ability of paralogs to promote the surface expression of FcRγ-dependent XFL2 was demonstrated. Expression analysis of the FcRγ and TCRζ duplicates did not reveal any significant differences in the tissue distribution of corresponding mRNA either in adults or during development. This is in contrast to zebrafish TcRζ and FcRγ duplicates, which exhibit differential expression (Yoder et al., 2007).

Unlike other models of the duplicated gene evolution, the protein dosage model suggests that an increased protein production may have an advantageous effect for the retention of functionally equivalent duplicated genes. This idea seems to be particularly relevant for WGD-derived paralogs that are involved in macro-molecular complexes (Innan and Kondrashov, 2010; Aury et al., 2006). In such a case, the retention is usually explained by a necessity to maintain a proper dosage balance among distinct components of a protein complex. In line with this idea, *X. laevis* genome has two gene copies of each of the TSS-coupled intracellular protein kinases ZAP70, Syk, and PI3K. As intracellular signaling is strictly dependent on protein dosage, the beneficial effect of correct stoichiometric relationships between TSS and downstream protein kinases would be highly probable. Furthermore, we demonstrated the presence of two duplicated *TCRα* loci in *X. laevis*. One of these is highly similar to the *TCRαδ* locus of *S. tropicalis* (Parra et al., 2010). The second locus seems to be truncated; it lacks both *Cδ* and *Vδ* genes and contains a single *TCR Cα* gene with a family of *Vα* genes.

Apart from *TCRα*, there is not much difference between *X. laevis* and *S. tropicalis* in the number of genes for the well-known ligand-binding partners of TSS. Both previous experimental studies (Courtet et al., 2001) and our genome-mining data show that *X. laevis* has a single *IgH* locus. The *TCR Cδ*, *Cβ* and *Cγ* duplicates appear to have been lost as well. Our genome analysis suggests a similar number of genes in the FCRL, SLAM, Siglec and LRC families in the two species. To fit these data with the increased protein production of TSS, we propose the involvement of some additional presently undefined conventional or non-conventional (Hamerman et al., 2009) TSS-associating proteins in *X. laevis*.

Further studies may shed more light on the functional significance of duplicated *TSS* and *TCRα* loci of *X. laevis*. Among the topics of interest is how BCR and TCR complexes are assembled in the presence of multiple subunits and if there is any selectivity in association of the TSS paralogs with Ig and TCR chains at a single cell level. The presence of two *TCRα* loci is to our knowledge a unique feature not found in other species. It is known that, in mammals, the *TCRα* gene rearrangement is not subjected to allelic exclusion. As a result, a fraction of mammalian T cells, in particular regulatory T cells (Tregs), may express two different TCRs (Tuovinen et al., 2006; Huang and Kanagawa, 2001; Petrie et al., 1993). The dual TCR expressing T cells remain poorly characterized, yet they have been suggested to play a role in T cell tolerance induction and autoimmunity. The presence of two functional *TCRα* loci in *X. laevis* may imply up to four different TCRs per cell in the absence of allelic and locus exclusion. It would be of interest to examine how *TCRα* rearrangements and expression are regulated in this amphibian species.

From an evolutionary perspective of relevance is that the TSS genes map to the paralogous chromosomal regions in the mammalian genome. As these regions are generally thought to represent footprints of two ancient vertebrate-specific WGDs, it could be hypothesized that the modern set of TSS genes might have arisen from a common ancestor. This idea is supported by a high similarity of the transmembrane regions of CD3ε/γ/δ and DAP10/12 (Call et al., 2010) and by some data showing the TSS expansion in tetraploid species (Mewes et al., 2009; Liu et al., 2008; Yoder et al., 2007; Alabyev et al., 2000). Our findings, together with the previous reports, show that long-term maintenance is a usual evolutionary fate for WGD-derived TSS paralogs. The ancient vertebrate tetraploidizations might have had a similar effect thereby providing a possibility for descendants of a hypothetical TSS-ancestor to structurally diverge and acquire novel functions. The dramatic expansion and diversification of immunoreceptor families that had happened in the early vertebrate evolution (Flajnik and Kasahara, 2010; Zucchetti et al., 2009; Du Pasquier et al., 2001; Kasahara et al., 1997) might have been a driving force behind the TSS paralog divergence and fixation.

Supplementary Material

Refer to Web version on PubMed Central for supplementary material.

Acknowledgments

IBR was supported by the Intramural Research Program of the National Library of Medicine at National Institutes of Health (US Department Health and Human Services).

JR and FDA were supported by grants from the National Institutes of Health (R24-AI-059830) and National Sciences Foundation (IOB-074271).

LG was supported by a LSRF PDF from the Howard Hughes Medical Institute.

AVT was supported by the Russian Basic Research Fund program 11-04-01165-a and by the Russian Academy of Sciences program “Molecular and Cellular Biology”, grant number 6.23.

Abbreviations

TSS	Transmembrane Signaling Subunits
ITAM	Immunoreceptor Tyrosine-based Activation Motif
WGD	whole genome duplication
CDS	Coding Sequence

References

Alabyev BY, Guselnikov SV, Najakshin AM, Mechetina LV, Taranin AV. CD3epsilon homologues in the chondrostean fish *Acipenserruthenus*. Immuno-genetics. 2000; 51:1012–1020.

Aury JM, Jaillon O, Duret L, Noel B, Jubin C, Porcel BM, Segurens B, Daubin V, Anthouard V, Aiach N, Arnaiz O, Billaut A, Beisson J, Blanc I, Bouhouche K, Camara F, Duharcourt S, Guigo R, Gogendeau D, Katinka M, Keller AM, Kissmehl R, Klotz C, Koll F, Le Mouel A, Lepere G, Malinsky S, Nowacki M, Nowak JK, Plattner H, Poulain J, Ruiz F, Serrano V, Zagulski M, Dessen P, Betermier M, Weissenbach J, Scarpelli C, Schachter V, Sperling L, Meyer E, Cohen J, Wincker P. Global trends of whole-genome duplications revealed by the ciliate Paramecium tetraurelia. Nature. 2006; 444:171–178. [PubMed: 17086204]

Barrow AD, Trowsdale J. The extended human leukocyte receptor complex: diverse ways of modulating immune responses. Immunol Rev. 2008; 224:98–123. [PubMed: 18759923]

Call ME, Wucherpfennig KW, Chou JJ. The structural basis for intra-membrane assembly of an activating immunoreceptor complex. Nat Immunol. 2010; 11:1023–1029. [PubMed: 20890284]

Chain FJ, Evans BJ. Multiple mechanisms promote the retained expression of gene duplicates in the tetraploid frog Xenopus laevis. PLoS Genet. 2006; 2:e56. [PubMed: 16683033]

Chida AS, Goyos A, Robert J. Phylogenetic and developmental study of CD4, CD8 α and β T cell co-receptor homologs in two amphibian species, Xenopus tropicalis and Xenopus laevis. Dev Comp Immunol. 2011; 35:366–377. [PubMed: 21075137]

Chretien I, Marcuz A, Fellah J, Charlemagne J, Du Pasquier L. The T cell receptor beta genes of Xenopus. Eur J Immunol. 1997; 27:763–771. [PubMed: 9079820]

Colonna M. DAP12 signaling: from immune cells to bone modeling and brain myelination. J Clin Invest. 2003; 111:313–314. [PubMed: 12569153]

Courtet M, Flajnik M, Du Pasquier L. Major histocompatibility complex and immunoglobulin loci visualized by in situ hybridization on Xenopus chromosomes. Dev Comp Immunol. 2001; 25:149–157. [PubMed: 11113284]

Du Pasquier L, Zucchetti I, De Santis R. Immunoglobulin superfamily receptors in protochordates: before RAG time. Immunol Rev. 2001; 198:233–248. [PubMed: 15199966]

Dzialo RC, Cooper MD. An amphibian CD3 homologue of the mammalian CD3 gamma and delta genes. Eur J Immunol. 1997; 27:1640–1647. [PubMed: 9247572]

Evans BJ. Genome evolution and speciation genetics of clawed frogs (Xen-opus and Silurana). Front Biosci. 2008; 13:4687–4706. [PubMed: 18508539]

Fernández A, Tzeng YH, Hsu SB. Subfunctionalization reduces the fitness cost of gene duplication in humans by buffering dosage imbalances. BMC Genomics. 2011; 12:604. [PubMed: 22168623]

Flajnik MF, Kasahara M. Origin and evolution of the adaptive immune system: genetic events and selective pressures. Nat Rev Genet. 2010; 11:47–59. [PubMed: 19997068]

Flajnik MF, Tlapakova T, Criscitiello MF, Krylov V, Ohta Y. Evolution of the B7 family: co-evolution of B7H6 and NKp30, identification of a new B7 family member, B7H7, and of B7's historical relationship with the MHC. Immunogenetics. 2012; 64:571–590. [PubMed: 22488247]

Gobel TW, Meier EL, Du Pasquier L. Biochemical analysis of the Xenopuslaevis TCR/CD3 complex supports the "stepwise evolution" model. Eur J Immunol. 2000; 30:2775–2781. [PubMed: 11069057]

Guselnikov SV, Laktionov PP, Najakshin AM, Baranov KO, Taranin AV. Expansion and diversification of the signaling capabilities of the CD2/SLAM family in Xenopodinae amphibians. Immunogenetics. 2011; 63:679–689. [PubMed: 21667045]

Guselnikov SV, Reshetnikova ES, Najakshin AM, Mechetina LV, Robert J, Taranin AV. The amphibians Xenopus laevis and Silurana tropicalis possess a family of activating KIR-related immunoglobulin-like receptors. Dev Comp Immunol. 2010; 34:308–315. [PubMed: 19896971]

Guselnikov SV, Ramanayake T, Erilova AY, Mechetina LV, Najakshin AM, Robert J, Taranin AV. The Xenopus FcR family demonstrates continually high diversification of paired receptors in vertebrate evolution. BMC Evol Biol. 2008; 8:148. [PubMed: 18485190]

Guselnikov SV, Bell A, Najakshin AM, Robert J, Taranin AV. Signaling FcRgamma and TCRzeta subunit homologs in the amphibian Xenopus laevis. Dev Comp Immunol. 2003a; 27:727–733. [PubMed: 12798368]

Guselnikov SV, Najakshin AM, Taranin AV. Fugurubripes possesses genes for the entire set of the ITAM-bearing transmembrane signal subunits. Immunogenetics. 2003b; 55:472–479. [PubMed: 12955357]

Haire RN, KitzanHaindfield MK, Turpen JB, Litman GW. Structure and diversity of T-lymphocyte antigen receptors alpha and gamma in Xenopus. Immunogenetics. 2002; 54:431–438. [PubMed: 12242593]

Hamerman JA, Ni M, Killebrew JR, Chu CL, Lowell CA. The expanding roles of ITAM adapters FcRgamma and DAP12 in myeloid cells. Immunol Rev. 2009; 232:42–58. [PubMed: 19909355]

Hellsten U, Harland RM, Gilchrist MJ, Hendrix D, Jurka J, Kapitonov V, Ovcharenko I, Putnam NH, Shu S, Taher L, Blitz IL, Blumberg B, Dichmann DS, Dubchak I, Amaya E, Detter JC, Fletcher R, Gerhard DS, Goodstein D, Graves T, Grigoriev IV, Grimwood J, Kawashima T, Lindquist E, Lucas SM, Mead PE, Mitros T, Ogino H, Ohta Y, Poliakov AV, Pollet N, Robert J, Salamov A, Sater AK, Schmutz J, Terry A, Vize PD, Warren WC, Wells D, Wills A, Wilson RK, Zimmerman LB, Zorn AM, Grainger R, Grammer T, Khokha MK, Richardson PM, Rokhsar DS. The genome of the Western clawed frog Xenopus tropicalis. Science. 2010; 328:633–636. [PubMed: 20431018]

Huang C, Kanagawa O. Ordered and coordinated rearrangement of the TCR alpha locus: role of secondary rearrangement in thymic selection. J Immunol. 2001; 166:2597–2601. [PubMed: 11160321]

Hughes AL. The evolution of functionally novel proteins after gene duplication. Proc Biol Sci. 1994; 256:119–124. [PubMed: 8029240]

Humphrey MB, Lanier LL, Nakamura MC. Role of ITAM-containing adapter proteins and their receptors in the immune system and bone. Immunol Rev. 2005; 208:50–65. [PubMed: 16313340]

Innan H, Kondrashov F. The evolution of gene duplications: classifying and distinguishing between models. Nat Rev Genet. 2010; 11:97–108. [PubMed: 20051986]

Ivashkiv LB. Cross-regulation of signaling by ITAM-associated receptors. Nat Immunol. 2009; 10:340–347. [PubMed: 19295630]

James-Zorn C, Ponferrada VG, Jarabek CJ, Burns KA, Segerdell EJ, Lee J, Snyder K, Bhattacharyya B, Karpinka JB, Fortriede J, Bowes JB, Zorn AM, Vize PD. Xenbase: expansion and updates of the Xenopus model organism database. Nucleic Acids Res. 2013; 41:D865–D870. [PubMed: 23125366]

Kasahara M, Nakaya J, Satta Y, Takahata N. Chromosomal duplication and the emergence of the adaptive immune system. Trends Genet. 1997; 13:90–92. [PubMed: 9066265]

Kondrashov FA, Rogozin IB, Wolf YI, Koonin EV. Selection in the evolution of gene duplications. Genome Biol. 2002; 3:RESEARCH0008. [PubMed: 11864370]

Kuhns MS, Davis MM. Disruption of extracellular interactions impairs T cell receptor-CD3 complex stability and signaling. Immunity. 2007; 26:357–369. [PubMed: 17368054]

Liu Y, Moore L, Koppang EO, Hordvik I. Characterization of the CD3zeta, CD3gammadelta and CD3epsilon subunits of the T cell receptor complex in Atlantic salmon. Dev Comp Immunol. 2008; 32:26–35. [PubMed: 17532043]

Lynch M, Conery JS. The evolutionary fate and consequences of duplicate genes. Science. 2000; 290:1151–1155. [PubMed: 11073452]

Malissen B, Ardouin L, Lin SY, Gillet A, Malissen M. Function of the CD3 subunits of the pre-TCR and TCR complexes during T cell development. Adv Immunol. 1999; 72:103–148. [PubMed: 10361573]

Mewes J, Verheijen K, Montgomery BC, Stafford JL. Stimulatory catfish leukocyte immune-type receptors (IpLITRs) demonstrate a unique ability to associate with adaptor signaling proteins and participate in the formation of homo- and heterodimers. Mol Immunol. 2009; 47:318–331. [PubMed: 19800691]

Niiro H, Clark EA. Regulation of B-cell fate by antigen-receptor signals. Nat Rev Immunol. 2002; 2:945–956. [PubMed: 12461567]

Ohno, S. Evolution by Gene Duplication. Springer-Verlag; New York: 1970.

Ohta Y, Goetz W, Hossain MZ, Nonaka M, Flajnik MF. Ancestral organization of the MHC revealed in the amphibian Xenopus. J Immunol. 2006; 176:3674–3685. [PubMed: 16517736]

Parra ZE, Ohta Y, Criscitiello MF, Flajnik MF, Miller RD. The dynamic TCRdelta: TCRdelta chains in the amphibian Xenopus tropicalis utilize antibody-like V genes. Eur J Immunol. 2010; 40:2319–2329. [PubMed: 20486124]

Pegueroles C, Laurie S, Alba MM. Accelerated evolution after gene duplication: a time-dependent process affecting just one copy. Mol Biol Evol. 2013; 30:1830–1842. [PubMed: 23625888]

Petrie HT, Livak F, Schatz DG, Strasser A, Crispe IN, Shortman K. Multiple rearrangements in T cell receptor alpha chain genes maximize the production of useful thymocytes. J Exp Med. 1993; 178:615–622. [PubMed: 8393478]

Radaev S, Zou Z, Tolar P, Nguyen K, Nguyen A, Krueger PD, Stutzman N, Pierce S, Sun PD. Structural and functional studies of Igalphabeta and its assembly with the B cell antigen receptor. Structure. 2010; 18:934–943. [PubMed: 20696394]

Reth M. Antigen receptor tail clue. Nature. 1989; 338:383–384. [PubMed: 2927501]

Robinson-Rechavi M, Huchon D. RRTree: relative-rate tests between groups of sequences on a phylogenetic tree. Bioinformatics. 2000; 16:296–297. [PubMed: 10869026]

Rogozin IB. Complexity of gene expression evolution after duplication: protein dosage rebalancing. Genet Res Int. 2014:516508. [PubMed: 25197576]

Shores EW, Ono M, Kawabe T, Sommers CL, Tran T, Lui K, Udey MC, Ravetch J, Love PE. T cell development in mice lacking all T cell receptor zeta family members (Zeta, eta, and FcepsilonRIgamma). J Exp Med. 1998; 187:1093–10101. [PubMed: 9529325]

Shum BP, Avila D, Du Pasquier L, Kasahara M, Flajnik MF. Isolation of a classical MHC class I cDNA from an amphibian. Evidence for only one class I locus in the Xenopus MHC. J Immunol. 1993; 151:5376–5386. [PubMed: 8228232]

Takai T, Li M, Sylvestre D, Clynes R, Ravetch JV. FcR gamma chain deletion results in pleiotrophic effector cell defects. Cell. 1994; 76:519–529. [PubMed: 8313472]

Tamura K, Dudley J, Nei M, Kumar S. MEGA4: Molecular Evolutionary Genetics Analysis (MEGA) software version 4.0. Mol Biol Evol. 2007; 24:1596–1599. [PubMed: 17488738]

Timberlake, KC. Chemistry. 5. Haper-Collins Publishers Inc; New York: 1992.

Tuovinen H, Salminen JT, Arstila TP. Most human thymic and peripheral-blood CD4+ CD25+ regulatory T cells express 2 T-cell receptors. Blood. 2006; 108:4063–4070. [PubMed: 16926292]

Viertlboeck BC, Schmitt R, Hanczaruk MA, Crooijmans RP, Groenen MA, Gobel TW. A novel activating chicken IgYFcR is related to leukocyte receptor complex (LRC) genes but is located on a chromosomal region distinct from the LRC and FcR gene clusters. J Immunol. 2009; 182:1533–1540. [PubMed: 19155501]

Yoder JA, Orcutt TM, Traver D, Litman GW. Structural characteristics of zebrafishorthologs of adaptor molecules that associate with transmembrane immune receptors. Gene. 2007; 401:154–164. [PubMed: 17719728]

Zhao Y, Pan-Hammarstrom Q, Yu S, Wertz N, Zhang X, Li N, Butler JE, Hammarstrom L. Identification of IgF, a hinge-region-containing Ig class, and IgD in Xenopus tropicalis. Proc Natl Acad Sci U S A. 2006; 103:12087–12092. [PubMed: 16877547]

Zucchetti I, De Santis R, Grusea S, Pontarotti P, Du Pasquier L. Origin and evolution of the vertebrate leukocyte receptors: the lesson from tunicates. Immunogenetics. 2009; 61:463–481. [PubMed: 19404636]

Appendix A. Supplementary data

Supplementary data related to this article can be found at http://dx.doi.org/10.1016/j.dci.2015.07.002.

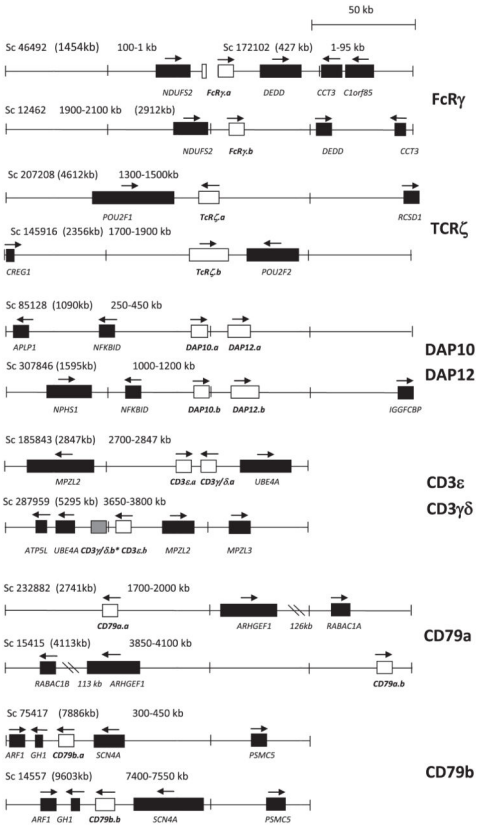

Fig. 1.

Schematic representation of scaffolds containing duplicated TSS genes. Scaffolds are from the *X. laevis* genome version 7.1. Headlines show the scaffold (Sc) number, the size of the scaffold (in parentheses) and the fragment coordinates on the scaffold. The bottom lines contain the gene designations according to their counterparts in the human genome. The TSS genes and their neighbors are shown by open and filled rectangles, respectively. Arrows show transcription orientation. The scaffold orientation corresponds to that in the Xenbase, except for the Sc 46492 that is presented in opposite orientation. The *MPZL2* and *MPZL3* genes on the scaffold 185843, CD3γ/δ* pseudogene (shown by gray rectangle) on scaffold 287959 and DAP10.b gene on scaffold 307846 were absent from the Xenbase annotation at the moment of our search. Double slash indicates a gap with a size shown in the corresponding bottom lines.

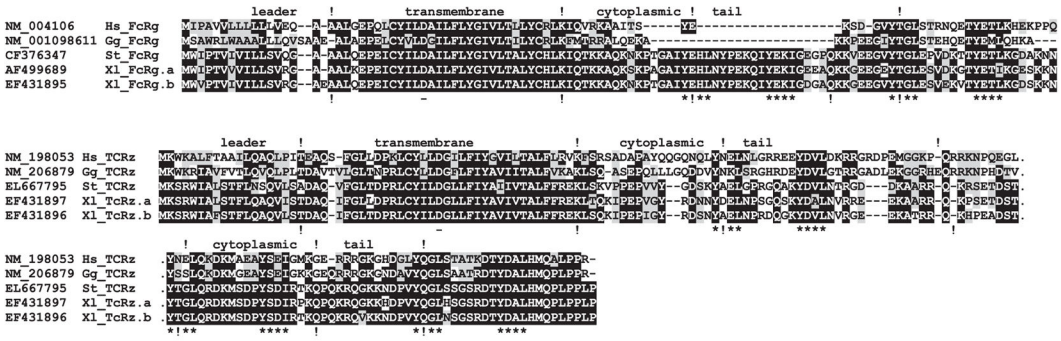

Fig. 2.

Multiple alignment of the deduced amino acid sequences of *Xenopus laevis* (Xl), *Silurana tropicalis* (St), chicken (Gg) and human (Hs) FcRγ and TcRζ subunits. Identical amino acid residues are denoted by white letters on black background, conserved residues – by black letters on gray background. Dashes designate gaps introduced for sequence alignments. Exclamation marks indicate exon-intron boundaries in human (upper line) and *X. laevis* (bottom line) genes. Asterisks designate ITAMs. Minus designates conserved negatively charged amino acid residue in the TM region.

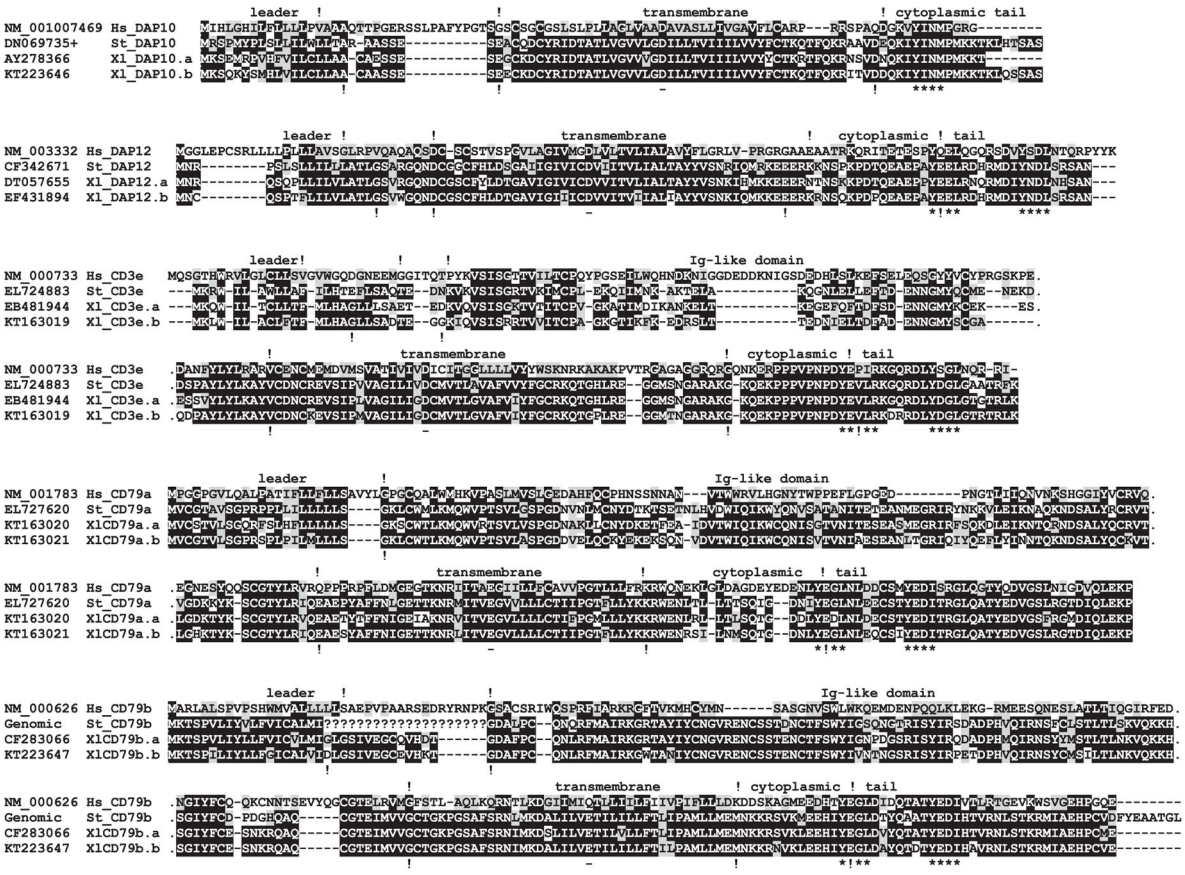

Fig. 3.

Multiple alignment of the deduced amino acid sequences of *Xenopus laevis* (Xl), *Silurana tropicalis* (St), and human (Hs) DAP10, DAP12, CD3 and CD79 subunits. Identical amino acid residues are denoted by white letters on black background, conserved residues – by black letters on gray background. Dashes designate gaps introduced for sequence alignments. Exclamation marks indicate exon-intron boundaries in human (upper line) and *X. laevis* (bottom line) genes. Asterisks designate tyrosine-based motifs. Minus designates conserved negatively charged amino acid residue in the TM region. St_DAP10 sequence was deduced using *S. tropicalis* genomic sequence along with EST cDNA sequences DN069735 and EL728268.

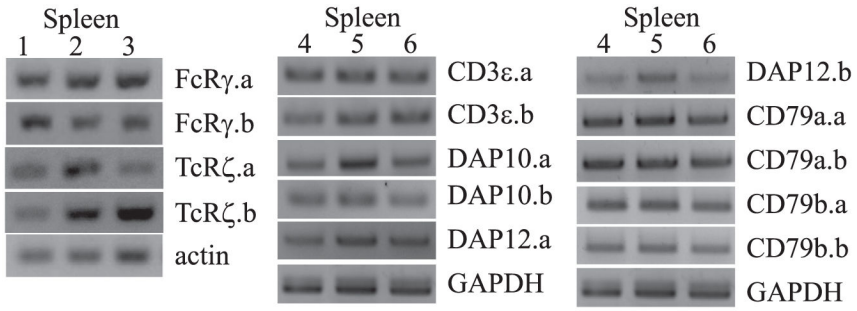

Fig. 4.

RT-PCR analysis of mRNA coding for *X. laevis* TSS. Individual spleens of 6-month old adults were used for the analysis. The cDNA samples were normalized according to *GAPDH* or β-actin expression.

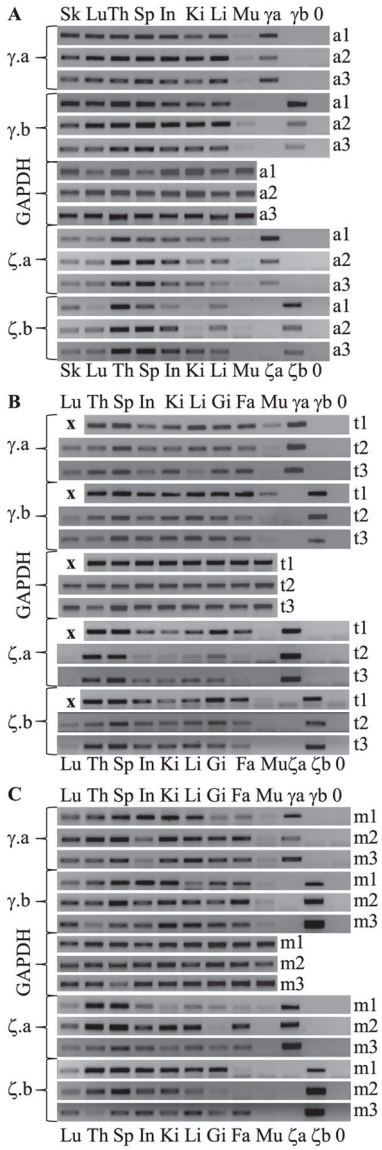

Fig. 5.

RT-PCR analysis of FcRγ.a/b and TcRζ.a/b mRNA from *X. laevis* tissues of 6-month old adult (A), stage 56 tadpole (B) and stage 61–64 metamorphic (C) animals. Three individuals at each stage (a/t/m1-3) were used. Tissues analyzed were: Skin, Lung, Thymus, Spleen, Intestine, Kidney, Liver, Gills, Fat body and Muscles. All cDNA samples were normalized according to *GAPDH* expression. Either 0.1 pg of plasmid with corresponding cDNA insert (γa, γb, ζa, ζb) or clear water (0) were used as controls. “x” denotes reactions that were not carried out.

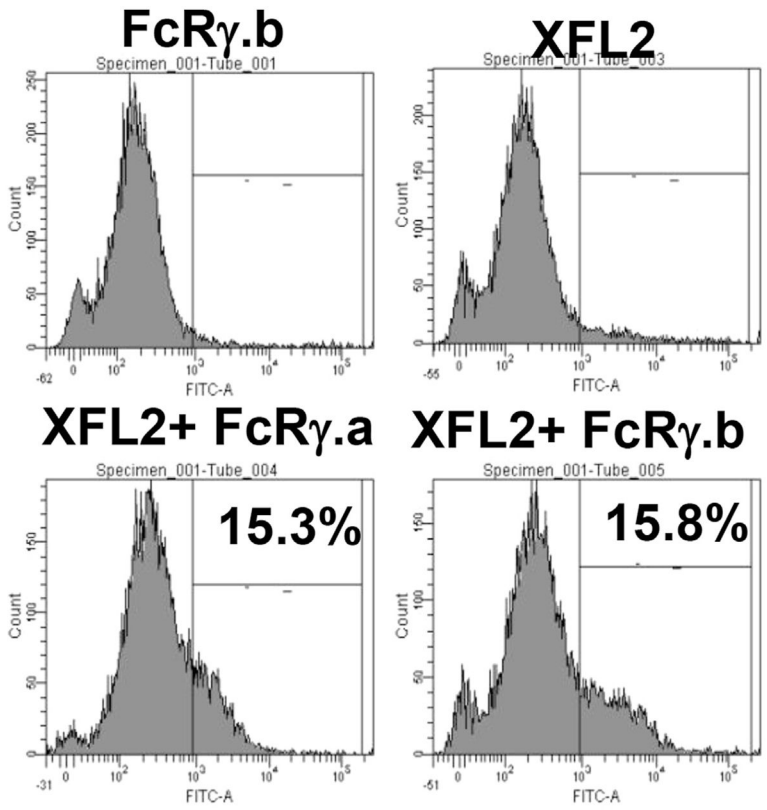

Fig. 6.

Flow cytometry analysis of living 293T cells co-transfected with plasmids encoding HA-tagged *X. laevis* XFL2 receptor and c-myc-tagged *X. laevis* FcRγ.a/b transmembrane signaling subunits. The cells were stained with anti-HA antibodies and analyzed with a BD FACSCanto II cytometer and the BD FACSDiva software.

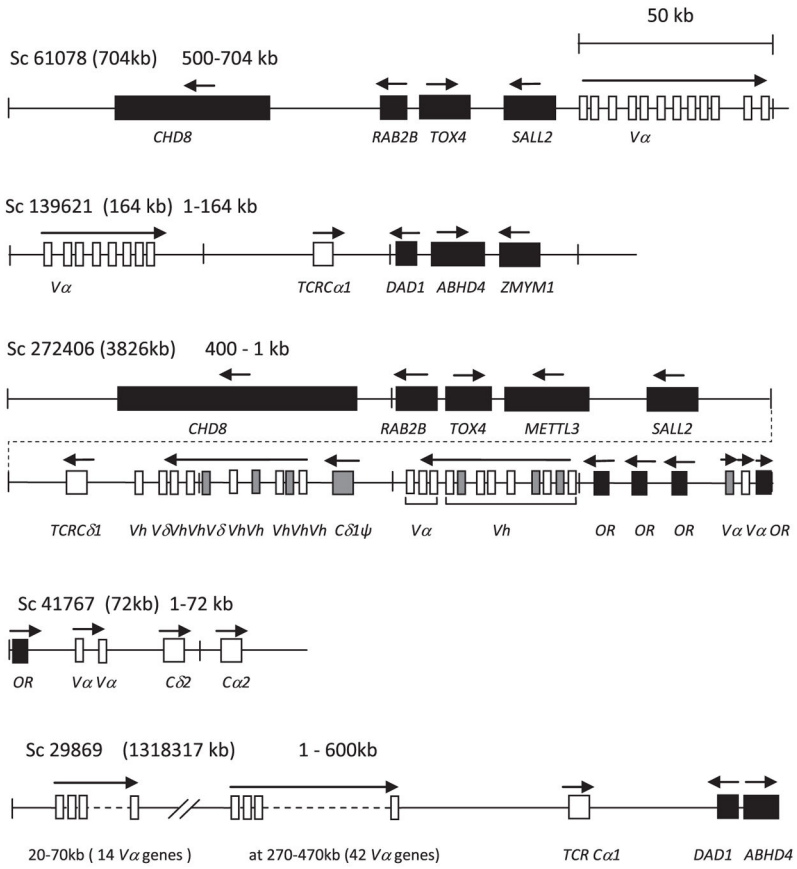

Fig. 7.

Schematic representation of scaffolds fragments containing *TCR* genes. Headlines show the scaffold (Sc) number, the size of the scaffold (in parentheses) and the fragment coordinates on the scaffold. The bottom lines contain designations of the genes according to their counterparts in the human genome. The *TCR* genes and their neighbors are shown by open and filled rectangles, respectively. Pseudogenes are shown by gray rectangles. Arrows show transcription orientation. Double slash indicates a gap with a size shown in the corresponding bottom lines.

Table 1

Relative rate test of paralogous genes in *Xenopus laevis*.

Gene name	Difference in rates of non-synonymous substitutions	Standard deviation	Probability
CD3e	0.036	0.023	0.11
CD79a	0.011	0.019	0.57
CD79b	0.012	0.012	0.32
DAP10	0.033	0.025	0.19
DAP12	0.005	0.022	0.83
FcRg	0.023	0.015	0.13
TCRz	0.017	0.015	0.26

The RRTREE program was used to estimate rates of non-synonymous substitutions (the PBL model was used) (Robinson-Rechavi and Huchon, 2000) between pairs of *Xenopus laevis* paralogous genes. *Silurana tropicalis* orthologs were used as outgroup sequences.